

Tissint among the shergottites: Parental melt composition, redox state, La/Yb and V/Sc. C. D. K. Herd¹, M. J. M. Duke², C. D. Bryden¹ and D. G. Pearson¹, ¹Department of Earth and Atmospheric Sciences, 1-26 Earth Sciences Building, University of Alberta, Edmonton, Alberta, T6G 2E3, Canada, herd@ualberta.ca. ²SLOWPOKE Nuclear Reactor Facility, 2-51 South Academic Building, University of Alberta, Edmonton, Alberta, T6G 2G7, Canada.

Introduction: Tissint is an olivine-phyric shergottite with similarities to EETA79001 Lithology A in petrography and bulk composition [1]. As the first fall of a martian meteorite since Zagami (1962), Tissint represents a rare opportunity to study a relatively fresh sample of Mars.

Tissint consists of < 2 mm olivine megacrysts in a groundmass of compositionally zoned pyroxene and maskelynite, with accessory chromite, titanomagnetite, ilmenite, pyrrhotite, apatite and merrillite [e.g., 1]. Pyroxene consists of orthopyroxene cores, and pigeonite or augite rims [1]. Tissint's petrogenesis is similar to that inferred for other olivine-phyric shergottites; namely, precipitation of olivine megacrysts at some depth, followed by groundmass crystallization upon eruption near the martian surface. Olivine megacrysts are at minimum cumulate, if not xenocrystic.

Here we report on the SiO₂ content of Tissint bulk powders determined by Neutron Activation Analysis (NAA) at the SLOWPOKE Nuclear Reactor Facility, estimate the Tissint parent melt composition, provide an assessment of the redox conditions of crystallization obtained by oxybarometry, and compare Tissint to other shergottites.

Materials and methods: All analyses were carried out using the 58.25 g Tissint specimen from the University of Alberta Meteorite Collection (MET11640), which was cut using a Buehler Isomet Lowspeed saw with wafering blades. All cutting was done without lubrication, and cutting powders were retained for use as representative bulk material. NAA was carried out on three such powders (T1 = 0.2534 g, T4 = 0.0958 g, T7 = 0.2015 g). Silicon was determined by reactor fast NAA using a ¹⁰B-shield and the reaction ²⁹Si(n,p)²⁹Al. Brazilian quartz was used as a comparator standard.

Mineral compositions were obtained using a JEOL 8900 electron microprobe, operating using a focused (< 1 μm spot) at 15 kV and 20 nA. Standards were carefully selected, especially to ensure accurate analyses of chromite and ilmenite. Oxygen fugacity (*f*O₂) estimates were carried out using the CT Server olivine-pyroxene-spinel oxybarometer [2].

Results: The SiO₂ contents of the three samples are T1 = 44.95, T4 = 47.64, and T7 = 45.60 wt%, with an average value of 46.1 wt%. Correction for Cu contamination from the saw blade results in a value of 46.2 wt% SiO₂ which we take as our preferred value.

Several workers have noted variable modal abundances of olivine megacrysts in Tissint, likely as a result of 3-dimensional variability sampled by 2-dimensional sections. The degree of accumulation of olivine may be assessed by comparing the bulk Mg# with the predicted melt Mg# from the most magnesian olivine cores. The bulk Mg# of Tissint is 0.57; as far as we are aware, the most magnesian olivine is Fo₇₉, which would have been in equilibrium with melt of Mg# = 0.59, based on a Fe-Mg exchange $K_D = 0.35$ [3]. The discrepancy may be explained by accumulation of approximately 5% olivine. In Table 1 we report the bulk composition after [1], including our SiO₂ result, along with the calculated parental melt composition assuming removal of 5% olivine of Fo₇₉ – this is our preferred Tissint parental melt composition. The bulk composition of NWA 5789, a picritic melt, and the preferred parental melt composition of EETA79001 Lithology A groundmass (“Eg”), are shown for comparison. Tissint and Eg are similar in Mg#, although the differences in major element composition reflect Tissint's more picritic character. In contrast, the Tissint parental melt is very similar to the composition of NWA 5789, with the sole exception of FeO (and thus Mg#).

Table 1. Tissint bulk and parental melt compositions

	Tissint bulk	Tissint parental	NWA 5789 ^a	Eg ^b
SiO ₂	46.2	47.2	49.2	50.9
TiO ₂	0.63	0.67	0.48	0.52
Al ₂ O ₃	4.86	5.20	5.65	10.4
FeO	21.2	21.6	16.6	14.4
MnO	0.52	0.56	0.47	0.40
MgO	17.1	16.0	17.7	11.8
CaO	6.5	7.0	6.5	8.9
Na ₂ O	0.72	0.77	0.43	1.7
P ₂ O ₅	0.48	0.51	0.38	0.6
Total	98.2	99.5	97.4	99.99
Mg#	0.59	0.57	0.66	0.59
La/Yb	0.17	0.17	0.08	0.36

^aAfter [4]; ^bAfter [5].

Olivine cores in Tissint are not in compositional equilibrium with any reported pyroxene compositions, based on the ol/px Fe-Mg exchange $K_D = 1.2$ of [6]; the first pyroxenes to crystallize (~Wo₅En₆₅Fs₂₅; [1]) are in equilibrium with olivine of Fo₆₉ on this basis.

Estimates of fO_2 were carried out using these pairs along with selected low-Ti chromites ($0.47 < TiO_2 < 1.65$ wt%; $n = 10$). Results yield a wide range of temperatures, from 1474 to 775 °C, generally inversely correlating with TiO_2 , and a range of fO_2 , from $IW - 0.9$ to $IW + 0.8$. The wide ranges of estimates result from uncertainty as to which chromite is in equilibrium with the pyroxene and olivine. Our average fO_2 is $IW - 0.1 \pm 0.5$ log units, or $QFM - 3.8 \pm 0.4$.

Discussion: The low fO_2 of Tissint is consistent with its depleted incompatible trace element composition (e.g., low La/Yb); Tissint appears to maintain the relationship between redox state and incompatible trace elements observed in many other shergottites, and is grouped with other reduced and depleted members along with several other olivine-phyric shergottites (Figure 1). Although mineral equilibria-based fO_2 estimates have generally been interpreted as reflecting the magmatic conditions [7], this has been recently challenged by results from LAR 06319 [8] and the poikilitic shergottites [9], which suggest that the mantle sources of the shergottites fall within a more limited range, and that the most oxidized shergottites – as well as lithologies within shergottites – are the result of oxidation during ascent and eruption (red arrow in Figure 1).

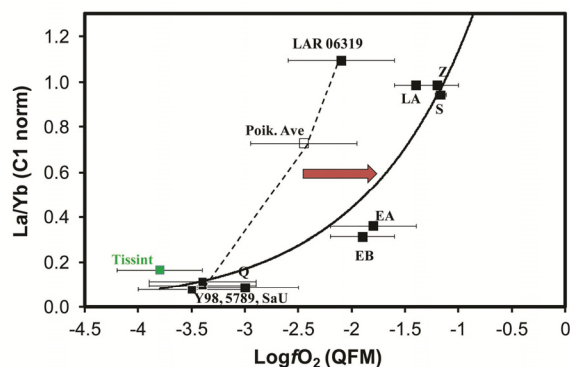


Figure 1. Plot of fO_2 (relative to the QFM buffer) vs. La/Yb ratio for select shergottites including Tissint. Solid line is best fit to all solid datapoints. Dashed line represents possible mantle source values. Poik. Ave. is the average poikilitic shergottite estimate of [9]. See text for discussion. Error bars on La/Yb are smaller than the symbol size.

Lee et al. [10] demonstrated that bulk rock V/Sc ratios can ‘see through’ effects of fractional crystallization, as well as magma ascent and differentiation, demonstrating that mid-ocean ridge basalts and arc lavas have similar V/Sc ratios and suggesting that the Earth’s upper mantle fO_2 is buffered to a limited range. The mantle sources of the shergottites presumably are not buffered in the same manner, since they likely reflect primitive redox reservoirs established during the

initial silicate differentiation of Mars [11]. Nevertheless, if the mineral equilibria-based fO_2 estimates for the shergottites reflect the redox states of the mantle sources, as opposed to the overprinting effects of ascent/degassing, then V/Sc should correlate with fO_2 . This does appear to be the case, with the basaltic shergottites (those without olivine phenocrysts), as well as the oxidized groundmasses of LAR 06319 and NWA 1068 forming a trend that overlaps with the relationship established by [10] (Fig. 2). The overlap strongly suggests that the oxygen fugacities of these lithologies reflect the redox states of their mantle sources.

In contrast, however, the fO_2 of the olivine-phyric shergottites do not correlate with the basaltic shergottites, grouping at low fO_2 and high V/Sc ratio. The offset cannot be explained by fractionation of olivine or spinel; nor can it be explained by differing amounts of partial melting of the source, to which V/Sc is relatively insensitive at $fO_2 < QFM$ [10]. We suggest instead that olivine-phyric and basaltic shergottites are derived from distinct mantle sources.

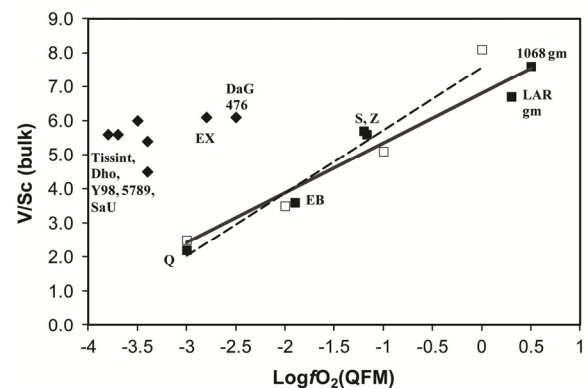


Figure 2. Plot of fO_2 vs. V/Sc for select basaltic (squares) and ol-phyric (diamonds) shergottites. Dashed line and open squares after [10]. Abbreviations as in Fig. 1; EX = EETA79001 lithology A xenocrysts. Error bars on V/Sc are smaller than the symbol size; see Fig. 1 for errors on fO_2 .

Acknowledgements: Funding for this research was provided by NSERC Grant 261740-08 to C.D.K.H. and a CERC grant to D.G.P.

References: [1] Aoudjehane H.C. et al. (2012) *Science*, 338, 785-788. [2] CT Server Ol-Px-Sp. http://ctserver.ofm-research.org/Olv_Spn_Opx/index.php. [3] Filiberto J. and Dasgupta R. (2011) *EPSL*, 304, 527-537. [4] Gross J. et al. (2011) *M&PS*, 46, 116-133. [5] Jones J.H. and Hanson B. (2011) *LPS XLII*, Abstract #2095. [6] Longhi J. and Pan V. (1989) *Proc. 19th LPSC*, 451-464. [7] Herd C.D.K. et al. (2002) *GCA*, 66, 2025-2036. [8] Peshier A.H. et al. (2010) *GCA*, 74, 4543-4576. [9] Walton E.L. et al. (2012) *M&PS*, 47, 1449-1474. [10] Lee C.T.A. et al. (2005) *J. Petrol.*, 46, 2313-2336. [11] Herd C.D.K. (2003) *M&PS*, 38, 1793-1805.